International Journal of ENGINE RESEARCH

Special Issue Article

International J of Engine Research
2015, Vol. 16(5) 627–638

DOI: 10.1177/1468087415594951
jer.sagepub.com
SAGE

Combustion and emission behavior of linear C_8-oxygenates

Benedikt Heuser, Peter Mauermann, Rajendra Wankhade, Florian Kremer and Stefan Pischinger

Abstract

Alternative fuels have become of great importance in order to secure a sustainable mobility within the next decades. Within the Cluster of Excellence, "Tailor-Made Fuels from Biomass" at RWTH Aachen University, several possible fuel candidates could be derived from (hemi-)cellulose by selective catalytic conversion. The proposed fuel candidates include furans, ethers, alcohols, and ketones. Experiments with the isomers di-n-butyl ether and 1-octanol have proven their suitability for diesel-type combustion. With di-n-butyl ether being prone to auto-ignition, overall hydrocarbon, carbon monoxide, and soot emissions are reduced compared to diesel. In contrast, the prolonged ignition delay with 1-octanol causes an increase in HC and CO emissions particularly at low engine loads. However, soot emissions are even below those of di-n-butyl ether. With regard to particulate matter, an Exhaust Emissions Particulate Sizer Spectrometer (EEPS™) has been utilized to investigate the particle size or number distribution. Compared to diesel, a reduction of the total particle number up to 80% was seen with the oxygenates next to a shift toward reduced particle mobility diameter. The HC emissions of both di-n-butyl ether and 1-octanol have been studied in detail by means of gas chromatography–mass spectrometry. As a main result, not only the general emission reduction potential of the biofuel alternatives 1-octanol and di-n-butyl ether can be shown with this work. Gas chromatography–mass spectrometry revealed that the composition of hydrocarbons emitted with the C_8-oxygenates is almost equal to those with diesel, except for the unburned fuel that is present in the exhaust gas. Quantification showed that the carcinogenic component 1,3-butadiene increased with the alternative fuel candidates, whereas particularly benzene and ethyl benzene reduced. Since both di-n-butyl ether and 1-octanol are found in high proportions in the exhaust gas, the effects on the aftertreatment system have to be investigated in a subsequent campaign.

Keywords

Diesel combustion, oxygenated fuels, hydrocarbon emissions, particulate matter

Date received: 30 September 2014; accepted: 29 May 2015

Introduction

Increasing sensitivity for the environment as well as rising fuel prices have led to intense research activities on biofuels within the last decade. However, in particular, first-generation biofuels use corn and fruits as feedstock, and thus, the fuels directly compete with the food chain. In order to thoroughly investigate the whole process chain of new biofuels, the so-called Cluster of Excellence (CoE) "Tailor-Made Fuels from Biomass" (TMFB) was established in 2007 at RWTH Aachen University, as part of the Excellence Initiative funded by the German government to promote fundamental research at German universities. One of the overall aims of this CoE is to develop sustainable fuels for modern engines, both spark ignited (SI) and compression ignited (CI). Since the fuel can only be sustainable if both production and combustion are favorable in ecological terms, the focus of this research is on fuels that can be derived from side stream products. Thus, the feedstock used consists of cellulose, hemicellulose, and lignin. Since the biomass conversion can be highly efficient, new production pathways including new technologies, such as selective catalysis and ionic liquids, are utilized.[1–4] Moreover, the fuels can contribute to a highly efficient and clean combustion by their chemical

Institute for Combustion Engines, RWTH Aachen University, Aachen, Germany

Corresponding author:
Benedikt Heuser, Institute for Combustion Engines, RWTH Aachen University, Forckenbeckstr. 4, 52074 Aachen, Germany.
Email: Heuser@vka.rwth-aachen.de

and physical characteristics. For this reason, the new fuels will differ significantly from today's fuels, which are based on fossil sources. In the recent past, many possible fuel candidates have already been proposed by this CoE and were successfully tested in engines.[5–8] For both CI and SI engines, an adapted oxygen content and high volatility is targeted in order to enable a good mixture formation and to reduce soot emissions. Moreover, for SI engines, a compact molecule structure is favorable to improve anti-knock behavior. Therefore, the investigated molecules include not only ring structures such as furans and tetrahydrofurans but also linear molecules such as alcohols, ethers, and ketones. This study focuses on the combustion and emission behavior of TMFB's most recent fuel candidates for CI engines: di-n-butyl ether (DNBE) and its isomer 1-octanol (1-OL), both being linear C_8-oxygenates. Those fuel candidates have been investigated by means of engine experiments, where special measurement instruments, such as an Engine Exhaust Particle Sizer Spectrometer (EEPS™), have been utilized for a more detailed analysis of the particulate emissions.

In the literature, a detailed characterization of HC emissions is given for blends of biodiesel (B100), diesel, and ethanol as well as gasoline blended with ethanol,[9–16] but no study on the effect of the linear C_8-oxygenates DNBE and 1-OL could be found. Payri et al.[15] have shown that with biodiesel, the total HC emissions as well as the carbon number of HC molecules in the exhaust gas decrease compared to fossil diesel. Merritt et al.[16] investigated the effect of diesel blended with ethanol. They found critical emissions as, for instance, formaldehyde and acetaldehyde increased with higher shares of ethanol. Yet, simultaneously 1,3-butadiene and methyl ethyl ketone were reduced. Ethanol emissions significantly increased compared to B0 fuel. Moreover, it was presented that benzene emissions are predominantly fuel born.[16] Thus, with the use of the pure components DNBE and 1-OL, a significant decrease in the concentration of such cyclic structures is expected. However, these aromatic compounds can also be generated during combustion by C_6 and C_7 molecules, but these are unlikely to occur particularly during DNBE combustion.

In this study, gas chromatography (GC) and mass spectrometry (MS) have been utilized to gain a profound knowledge of the gaseous emissions with the use of the C_8-oxygenates derived in the CoE. All results will be compared to the findings with conventional EN590 diesel fuel.

Experimental setup and methodology

Single-cylinder setup and load points

Test carrier. The engine used for these investigations is a single-cylinder engine (SCE) with a displacement of 0.39 L. The fuel injection equipment (FIE) is close to series production and state of the art, featuring an injection pressure of up to 220 MPa. The engine control unit is based on a Rich Client Platform (RCP) computer, enabling a free determination of the injection parameters and thus compensation of fuel effects. The engine features a maximum specific power output of 80 kW/L with peak firing pressures of 19 MPa. Due to intense charge air and exhaust gas recirculation (EGR), cooling the engine meets EU-6 Emission Legislation (EU-6) NO_x level, while simultaneously achieving low particulate matter (PM) emissions. The re-entrant piston bowl is ω-shaped and has a bowl volume of 21.6 cm^3. The squish height is 0.78 mm. More detailed information on this engine can be found in previous publications.[17,18] Table 1 summarizes the main specifications of the engine.

Load points. In this work, five load points (LPs) have been investigated, ranging from almost idle conditions up to high part load. The location of these LPs within the engine map is displayed by Figure 1.

In Table 2, the calibration for each LP is given. Except for the start of energizing (SOE), all boundary conditions are constant for all fuels. The SOE is adjusted according to the fuel characteristics in order to allow a constant center of combustion (CA50).

Table 1. Engine hardware specification.

	Unit	
Displacement	cm^3	390
Stroke	mm	88.3
Bore	mm	75
Compression ratio	–	15:1
Valves or cylinders	–	4
Maximum cylinder pressure	MPa	19.0
Fuel injection equipment	–	Bosch piezo common-rail system
Maximum injection pressure	MPa	220.0
Nozzle	–	8 holes, 109 μm hole diameter, 153° cone angle
Hydraulic nozzle flow rate (HFR)	cm^3/30 s	310 at 10.0 MPa
Boosting	–	Maximum 0.38 MPa absolute

Table 2. Engine calibration at all investigated load points.

Load point	Engine speed or engine load	Center of combustion (CA50; ° CA BTDC)	Rail pressure (MPa)	Boost pressure (MPa)	Charge air temperature (°C)	Exhaust gas backpressure (MPa)	EU-6 NO_x level (g/kW h)
1	n = 1200 r/min (IMEP = 0.26 MPa)	−8.0	35.0	0.105	27	0.185	0.2
2	n = 1500 r/min (IMEP = 0.43 MPa)	−6.6	72.0	0.107	25	0.113	0.2
3	n = 1500 r/min (IMEP = 0.68 MPa)	−5.8	90.0	0.15	30	0.160	0.2
4	n = 2280 r/min (IMEP = 0.94 MPa)	−9.2	140.0	0.229	35	0.239	0.4
5	n = 2400 r/min (IMEP = 1.48 MPa)	−10.8	180.0	0.26	45	0.280	0.6

IMEP: indicated mean effective pressure; BTDC: before top dead center.

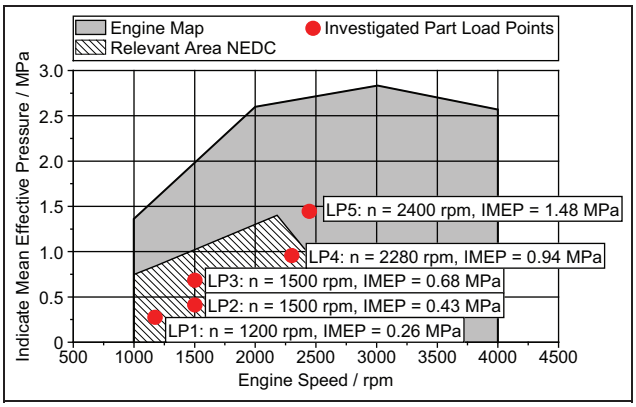

Figure 1. Engine map and investigated load points.
NEDC: New European Driving Cycle.

Thus, an influence on engine emission and efficiency by a retarded combustion, for instance, is prevented.

In particular, at low engine load and cold engine conditions, HC emissions are problematic. This is due to flame- and wall-quenching effects, leading to high HC emissions at engine-out. Moreover, at cold start conditions, the catalyst has not reached its light-off temperature. The combination of both effects results in very high tailpipe emissions. For this reason, investigations with the focus on HC emissions are often carried out at low engine temperatures.[9,19] Unfortunately, with 1-OL, a stable combustion at cold engine conditions could not be achieved with the hardware used in this very study. Hence, the HC emission spectra are presented at engine LPs 1 and 2 at warm engine conditions with engine oil and coolant temperature of 90 °C.

Measurement equipment

Regulated and unregulated emissions, that is, CO, CO_2, HC, NO_x, and PM, are measured at engine exhaust via these sampling systems:

- Total hydrocarbon (THC): flame ionization detector (FID; Rosemount NGA 2000);
- O_2: paramagnetic oxygen analyzer (Rosemount NGA 2000);
- CO: infrared gas analyzer (Rosemount NGA 2000);
- CO_2: infrared gas analyzer (Rosemount NGA 2000);
- NO_X: chemiluminescence analyzer (Eco Physics 700 EL ht);
- PM: filter paper method (AVL 415S).

Based on the measurement of the filter smoke number (FSN) by an AVL[20] 415 smoke meter, the indicated specific PM (ISPM) emissions can be calculated. During low-load operation, the extraction site for exhaust gas is located in the exhaust gas manifold. During medium- to high-load operation, it is placed downstream of the backpressure valve due to high exhaust gas backpressure. The lines are heated up to 205 °C for the HC, CO, and NO_x measurements to avoid condensation. The sample line of the smoke meter is heated to 75 °C. The EGR rate is calculated based on CO_2 concentration in the intake manifold. The fuel consumption is measured by a Coriolis-type fuel flow meter. An ultrasonic gas meter "FLowSic" by Sick is utilized to measure the air volume flow, which is calculated with the air temperature and its water content. The boost pressure can be adjusted independently by an external three-stage charging system, which also provides low intake air temperatures via three charge air coolers. An electric, position controlled EGR valve is used for adjusting the EGR rate. The exhaust gas backpressure is controlled by two valves and a bypass in the exhaust gas track in order to adjust the exhaust gas backpressure according to realistic values. For measuring the in-cylinder pressure, a water-cooled piezoelectric pressure transducer by Kistler (6041A) is utilized. FEV's "Combustion Analyzing System" (CAS) records the cylinder pressure as well as the intake and exhaust pressure signal. All pressures are recorded in steps of 0.5° crank angle (CA), except for the cylinder pressure, which is recorded at 0.1° CA. Indicated values, such as indicated mean effective pressure (IMEP), are recorded as an average of 50 cycles. The position of the crank angle and the differentiation between the high-pressure phase and the gas-exchange phase is measured by a crank angle sensor and an additional sensor at the intake camshaft. The ignition delay of the fuel is deduced from the time difference of the

in-cylinder pressure rise due to ignition (5% of fuel mass converted) and the start of fuel injection (SOI). The time lag between the injector SOE and SOI is 160 μs, being almost independent of the used fuel and injection pressure.

An EEPS by TSI is utilized in combination with the rotating disk thermodiluter 379020A and 379030 thermal conditioner for measuring particle size and number distribution within the range of 5.6–560 nm. Due to the complex structure of soot particles, the concentrations are given for the mobility particle diameter (D_p). The raw exhaust gas is sampled downstream of the backpressure valves, with the connecting line of exhaust track and diluter head being as short as possible. In order to keep the temperature history of the exhaust gas as simple as possible, the diluter head temperature is set to 150 °C. Within the thermal conditioner, the evaporation tubes are heated up to 350 °C in order to measure only the solid particle fraction.[21]

Exhaust gas samples for the gas chromatographic and mass spectrometric analysis are extracted approximately 250 cm downstream of the cylinder head flange via a 200-cm titan sampling tube with a water-cooled heat exchanger. For HC components ranging from C_2 to C_6, Carbosieve SIII tubes are used. The temperature at their inlet is 25 °C–27 °C. For long chained HC ranging from C_7 to C_{27}, Tenax GR tubes are utilized. Due to different temperature requirements, these have to be heated in a special furnace to 120 °C.

The sampled exhaust gas volume is calculated via the extraction time of 5 min and the calibrated flow of the SKC pump 224-PCXR8 of 40 mL/min. The analysis of the samples is performed using a PerkinElmer turbomatrix 350 thermal desorption injector, which is directly coupled to a thermo GC-MS system (GC: Agilent 7890A/MS: Agilent 5975 C MSD triple-axis detector). The Carbosieve or Tenax tubes are desorbed onto a multiphase condensation trap (PerkinElmer Air Toxic Trap cooled to −30 °C) during a time span of 3 min, at a temperature of 295 °C and a helium flow of 100 mL/min at closed inlet split. In the following step, the condensation trap is heated to 300 °C at a helium flow of 5 mL/min. All desorbed substances are injected into the gas chromatograph at closed outlet split with a helium excess pressure of 45 kPa. The temperatures of all transfer lines and valves amount to 225 °C. The gas chromatographic separation is performed in a 30-m Restek Rt-Q-Bond capillary column with an inside diameter (ID) of 320 μm for the Carbosieve tubes. In case of the Tenax GR tubes, a 60-m Restek Rxi-5 (ID = 250 μm) is used.

The temperature ramp of the Carbosieve SIII and Tenax tubes is different. For the Carbosieve tubes, the temperature control is set as follows: The start temperature of 40 °C is being held for 8 min and then heated up to 160 °C at a heating rate of 6 °C/min. From 160 °C onward, the temperature is increased by 15 °C/min until 240 °C is achieved. This temperature is held constant until the end of the separation. Since less volatile HCs are sampled with Tenax tubes, the temperature profile for separation is on a higher level than for Carbosieve SIII tubes: The start temperature of 40 °C is also held for 8 min, but heating up to 160 °C is slightly slower with 5 °C/min. The subsequent heat ramp to 270 °C shows a slope of 10 °C/min. Once 270 °C is held for 0.1 min, the subsequent heat ramp with 5 °C/min is started until the final separation temperature of 325 °C is reached.

The MS is performed in a mass range of 35–249 unified atomic mass units at a scan rate of 9 scans/s. The temperature of the mass spectrograph and the transfer lines are set to 200 °C and 240 °C, respectively.

Fuel characteristics

In addition to standard EN590 diesel fuel, the two isomers DNBE and 1-OL were investigated. Even though the chemical composition of both fuels is identical, the physical characteristics that are important for mixture formation and combustion are very different (see Table 3). Obviously, both 1-OL and DNBE differ significantly from diesel fuel. Both fuels feature a high oxygen content of 12.3% m/m, and thus, soot formation is expected to be reduced with respect to diesel fuel combustion. Moreover, the boiling point of both the C_8-oxygenates is at the lower end of the boiling curve of diesel fuel. However, the higher enthalpy of vaporization, its very low vapor pressure, and the increased

Table 3. Fuel characteristics.[23–25]

	Unit	Diesel	1-OL	DNBE
Boiling temperature	°C	180–350	195	141
Heating value	MJ/kg	42.9	38.4	38.4
Density	kg/m^3	833	830	770
Cetane number	–	56	~34[a]	~115[a]
Oxygen content	% m/m	0.14	12.3	12.3
Vapor pressure	Pa	< 100	12.5	640
Surface tension	mN/m	20.5	27.5	22.2
Dynamic viscosity	MPa s	3	5.8	0.64
Enthalpy of vaporization	kJ/kg	358	562	341

DNBE: di-n-butyl ether; 1-OL: 1-octanol.
[a]Derived cetane number (DCN).

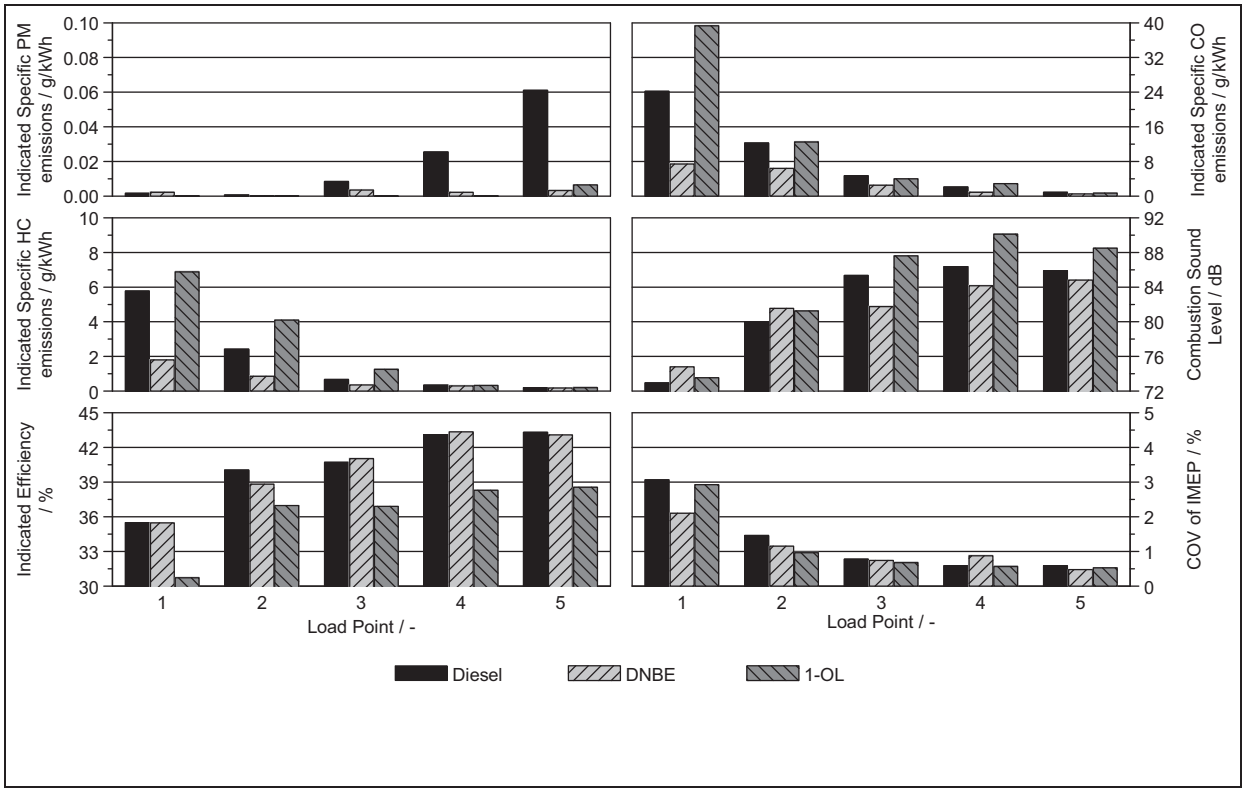

Figure 2. Indicated specific PM, CO, and HC emissions, combustion sound level (CSL), indicated efficiency, and standard deviation in IMEP for all three fuels at all five load points.

surface tension of 1-OL will cause an increase in liquid spray penetration as already presented by Jakob et al.[22] Since the longer ignition delay causes an enlargement of the gaseous mixing length, the overall equivalence ratio at the start of combustion is expected to be slightly lower when compared to diesel fuel. Contrary to 1-OL, its isomer DNBE is rather volatile and very prone to auto-ignition. Investigations have proven that the liquid core is short compared to diesel and 1-OL. Simultaneously, the initial ignition kernels are located significantly closer to the nozzle.[22]

Results and discussion

In the following, a brief discussion of the engine test results will be given with respect to the total HC and CO emissions, the efficiency, and the FSN measured for all three fuels in the five LPs. A more detailed particulate study by means of EEPS is introduced for the two highest LPs where PM emissions are most critical. A detailed discussion of all fuels at different compression ratios (CRs) was shown previously.[25] Below, the results of the detailed HC characterization are given only for the two lowest engine LPs since the higher temperatures at high engine load minimize the total HC emissions for all fuels. The color code used in this publication is black for findings with diesel, light gray for DNBE, and dark gray for 1-OL.

Thermodynamic results and PM emissions

In Figure 2, the ISPM, indicated specific CO (ISCO), and indicated specific HC (ISHC) emissions, the combustion sound level (CSL) as a measure for the combustion noise, the indicated efficiency, as well as the covariance (COV) of IMEP are displayed for all fuels. The engine load and speed increase from left to right. According to Table 2, the EGR rate was adjusted for all fuels to meet the EU-6 NO_x level at engine-out. The PM emissions increase with expanding load for diesel fuel. Here, the major impact of the alternative fuels becomes obvious: With both the C_8-oxygenates the PM emissions (based on FSN measurement) are significantly reduced in almost all LPs. In particular, at higher engine load, the PM emissions of diesel exceed those of the TMFB candidates up to 15-fold.

The impact of the fuel properties on the CO emission is shown in the upper right and on the HC emissions on the left of the second row. As expected, CO and HC emissions decrease for all fuels with higher load due to higher combustion temperature levels. Nevertheless, in LPs 1 and 2, the direct correlation between the fuel's reactivity and the ignition delay and the emissions can be seen: with DNBE igniting very fast, both HC and CO emissions are low since the fuel penetration at the start of ignition is rather short. Thus, wall- and flame-quenching effects are reduced to a minimum. In contrast, the fuel 1-OL shows a

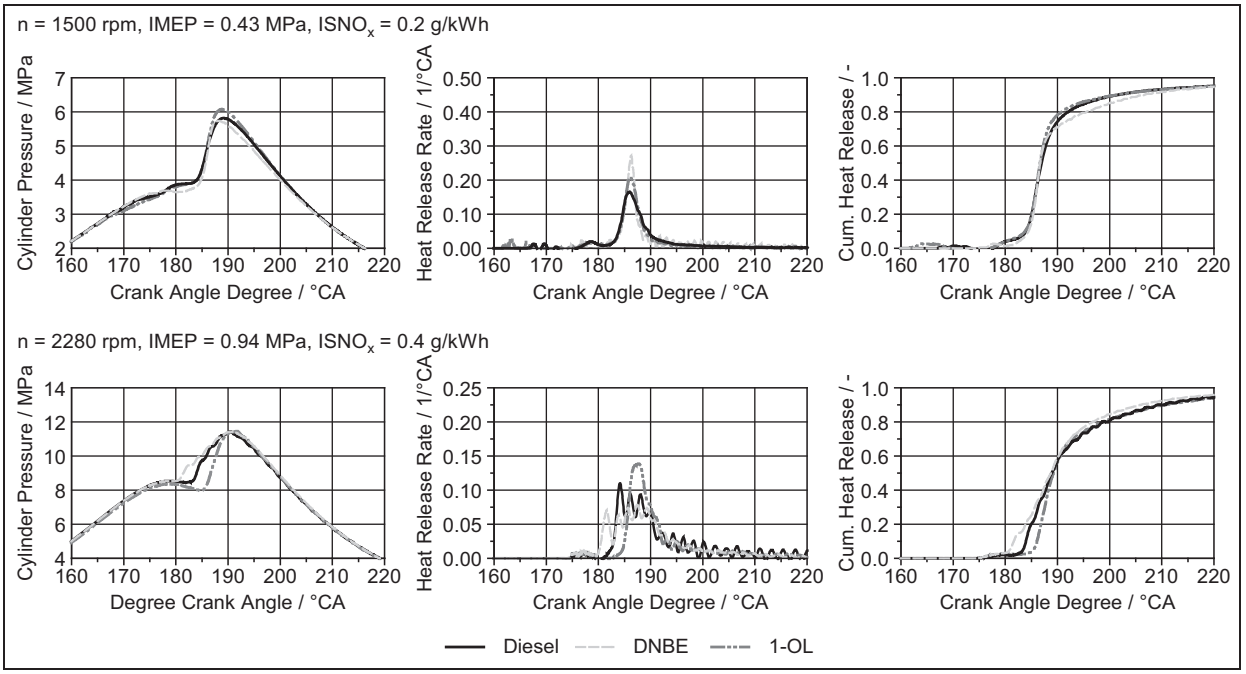

Figure 3. In-cylinder pressure, apparent heat release rate and cumulated (Cum.) heat release for all three fuels at the load points n = 1500 r/min (IMEP = 0.43 MPa) and at ISNO$_x$ = 0.2 g/kW h and n = 2280 r/min (IMEP = 0.94 MPa) and at ISNO$_x$ = 0.4 g/kW h.

significant elevation in CO emissions particularly in LP 1 compared to conventional diesel. However, the HC emissions are of the same magnitude in this LP. When looking at LP 2, it becomes obvious that HC and CO emissions are reduced compared to LP 1, but HC emissions with 1-OL exceed those with diesel by a factor 2.

On the right, in the center row, the CSL is depicted. Since the CA50 is kept constant (see Figure 3), the main driver for the combustion noise is the heat release rate. Due to higher rates of premixed burn, 1-OL shows the highest heat release rates in the LPs 3–5 (see Figure 3). However, due to a leaner combustion in the lowest LPs with 1-OL and diesel, the fuel with the highest reactivity shows the highest heat release rates. Thus, DNBE emits the highest combustion noise as indicated by the CSL.

On the lower left of Figure 2, the indicated efficiency is displayed. Since the CA50 is constant for all fuels (see Figure 3), there are only minor differences observed. These are caused mainly by varying combustion durations and thus varying wall heat losses due to different combustion temperatures. Only for LP 1, the slightly reduced efficiency with 1-OL might be induced by the elevated losses due to incomplete combustion that are caused by the high HC and CO emissions.

In the lower right, the COV of IMEP is shown. Even though the combustion of 1-OL at LP 1 is rather incomplete, the combustion stability is similar for all investigated fuels.

So far, the reduction of PM emissions was determined by FSN measurements only. However, since previous investigations have proven that oxygenated fuels may lead to different particle structures, the correlation of FSN to PM emissions might underestimate the total

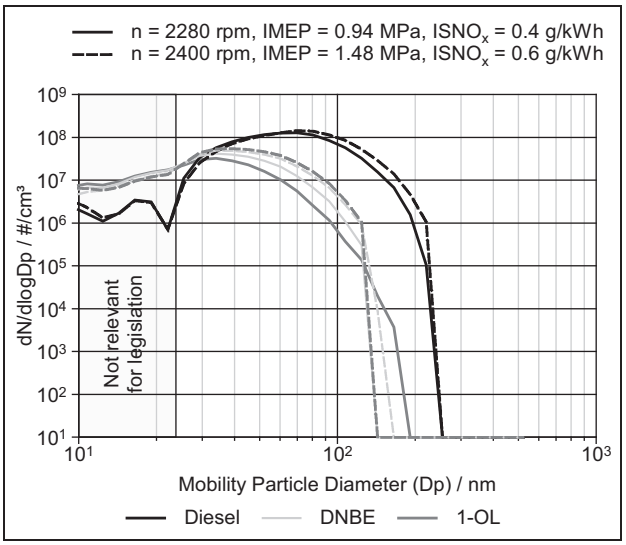

Figure 4. Particle size or number distribution for all three fuels at the load points n = 2280 r/min (IMEP = 0.94 MPa) and at ISNO$_x$ = 0.4 g/kW h and n = 2400 r/min (IMEP = 1.48 MPa) and at ISNO$_x$ = 0.6 g/kW h.

PM emissions with the C_8-oxygenates.[26–28] In order to investigate the PM emission in more detail, the particulate number to size distribution was measured using the EEPS. Since the relevance of PM emissions rises with increasing load, Figure 4 shows the results in the two highest LPs.

Overall, the FSN measurements are confirmed by EEPS measurements. With diesel fuel, the common size to number distribution with its peak at about D_p = 70 nm is observed. In between both LPs, the

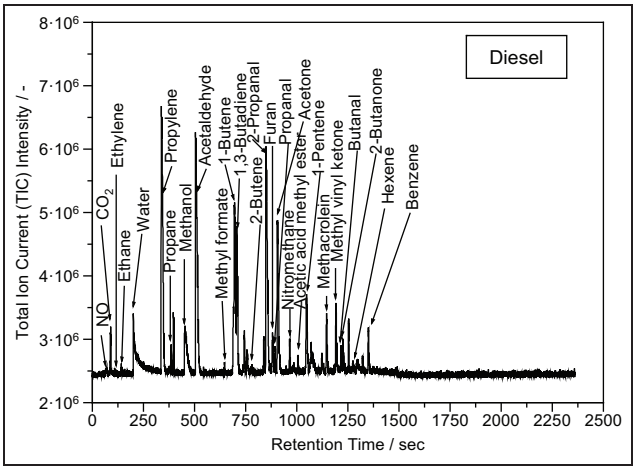

Figure 5. GC-MS HC emission spectra for diesel at n = 1200 r/min (IMEP = 0.26 MPa) and at EU-6 NO_x level (Carbosieve SIII).

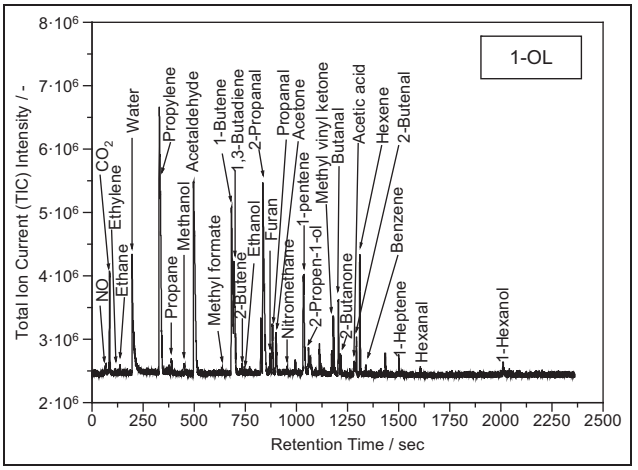

Figure 7. GC-MS HC emission spectra for 1-OL at n = 1200 r/min (IMEP = 0.26 MPa) and at EU-6 NO_x level (Carbosieve SIII).

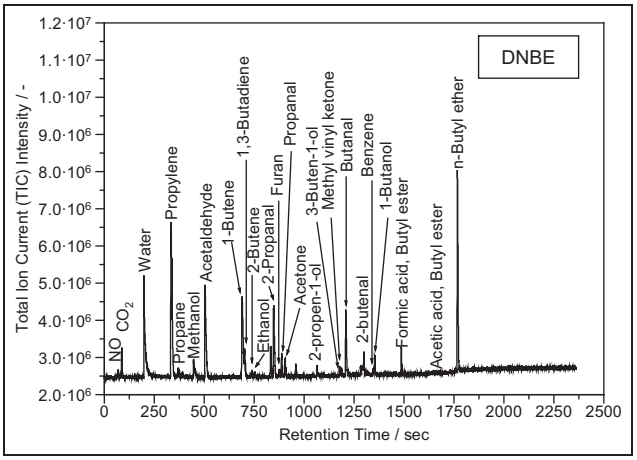

Figure 6. GC-MS HC emission spectra for DNBE at n = 1200 r/min (IMEP = 0.26 MPa) and at EU-6 NO_x level (Carbosieve SIII).

difference is rather low. The two oxygenates cause a drop in total particle number (PN): With conventional diesel, the total PN is up to fivefold of that of 1-OL. Moreover, a shift to smaller particle diameters is observed in both LPs for the C_8-oxygenates.

Hydrocarbon emission spectra

As discussed previously, the utilization of different fuel compositions will most likely alter the composition of the HC emissions in the exhaust gas. However, the standard technique for HC measurement is based on a FID, which is not able to distinguish between various HCs. Moreover, the response factor of the FID to different HC components can result in measurement errors, particularly if the emissions contain oxygenated molecules. Thus, a detailed assessment of HC emissions is not possible without knowing the exact composition of the exhaust gas.[29] With a Fourier transformation infrared (FTIR) spectrometer, a quantification of several species is possible. Yet, this requires a detailed knowledge of the HC composition a priori the tests due to overlap of the absorption peaks of different species.[30] For this reason, in this study, a measurement of the HC components by means of Carbosieve SIII and Tenax tubes was selected for exhaust gas sampling, even though these devices show slight drawbacks. With Carbosieve SIII and Tenax tubes, an assessment of the entire hydrocarbon spectrum is not possible. CH_4 cannot be adsorbed in the chosen temperature range, but CH_4 emissions can account for a significant part of the HC emissions. Moreover, polar components such as ketones and aldehydes are not measurable when occurring in extremely low concentrations in the parts per billion (ppb) range. Additionally, with the chosen sampling method via Carbosieve SIII and Tenax tubes, it cannot be ensured that all components are adsorbed with equal efficiency. Thus, the detected HC emissions cannot be recalculated into an absolute concentration in the raw exhaust gas. For this reason, the quantification that is presented in the next section could be made only on a qualitative basis. The emission spectra that were found by Carbosieve SIII tube for all fuels in the lowest LP 1 at n = 1200 r/min, IMEP = 0.26 MPa, are shown in Figures 5–7 and the corresponding measurements by Tenax tube in Figures 8–10. In the first row, the results with diesel fuel are presented, in the second, those with DNBE are shown, and in the last row, the GC-MS results with 1-OL are shown. For each fuel on the left, the Carbosieve SIII measurements are given and the corresponding Tenax measurements on the right. Analogous to the findings above, those in the higher LP at n = 1500 r/min (IMEP = 0.43 MPa) are given in Figures 11–16.

Independent of the investigated LP or the sample technique, for all three fuels investigated, almost the same HC species can be detected in the range up to C_7. However, in particular at low engine load conditions, the majority of the total HC emissions are caused by

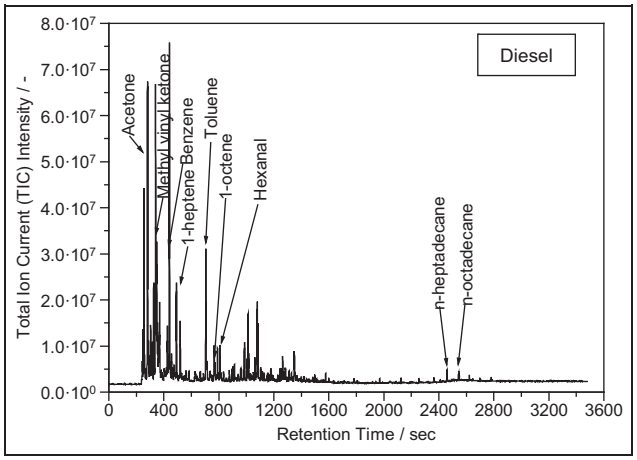

Figure 8. GC-MS HC emission spectra for diesel at n = 1200 r/min (IMEP = 0.26 MPa) and at EU-6 NO_x level (Tenax).

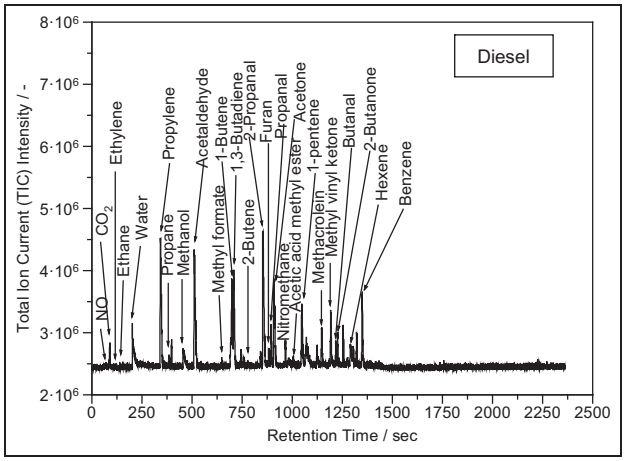

Figure 11. GC-MS HC emission spectra for diesel at n = 1500 r/min (IMEP = 0.43 MPa) and at EU-6 NO_x level (Carbosieve SIII).

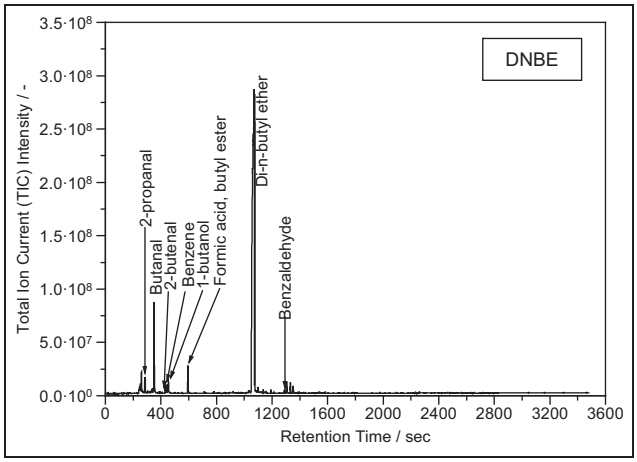

Figure 9. GC-MS HC emission spectra for DNBE at n = 1200 r/min (IMEP = 0.26 MPa) and at EU-6 NO_x level (Tenax).

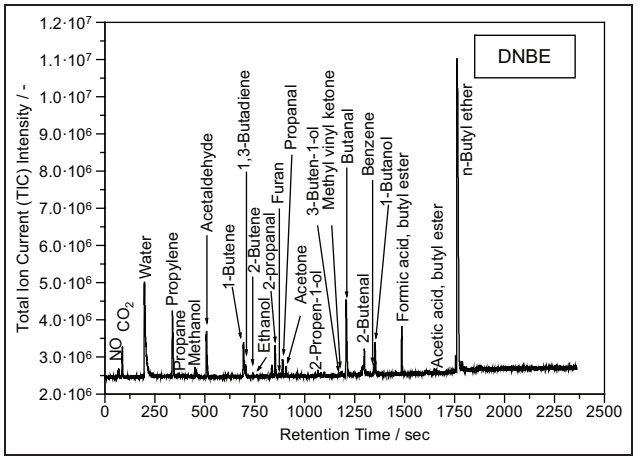

Figure 12. GC-MS HC emission spectra for DNBE at n = 1500 r/min (IMEP = 0.43 MPa) and at EU-6 NO_x level (Carbosieve SIII).

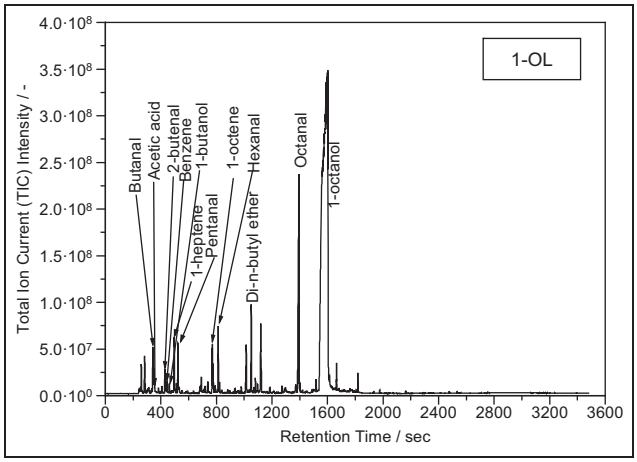

Figure 10. GC-MS HC emission spectra for 1-OL at n = 1200 r/min (IMEP = 0.26 MPa) and at EU-6 NO_x level (Tenax).

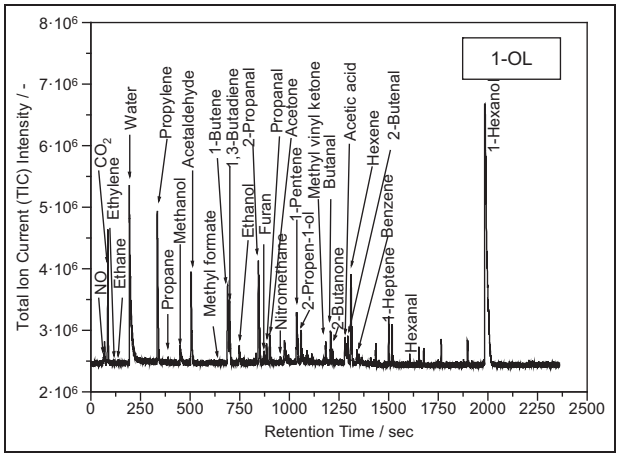

Figure 13. GC-MS HC emission spectra for 1-OL at n = 1500 r/min (IMEP = 0.43 MPa) and at EU-6 NO_x level (Carbosieve SIII).

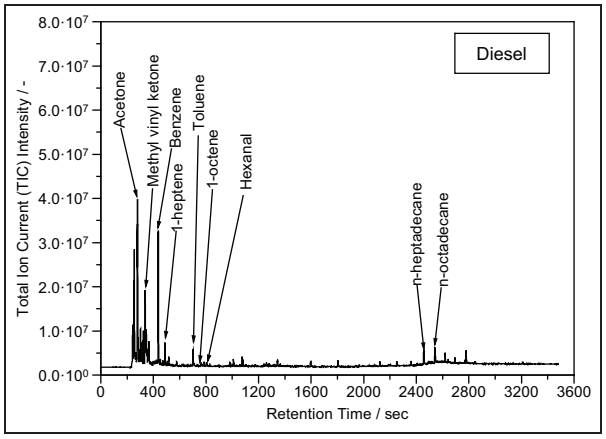

Figure 14. GC-MS HC emission spectra for diesel at n = 1500 r/min (IMEP = 0.43 MPa) and at EU-6 NO_x level (Tenax).

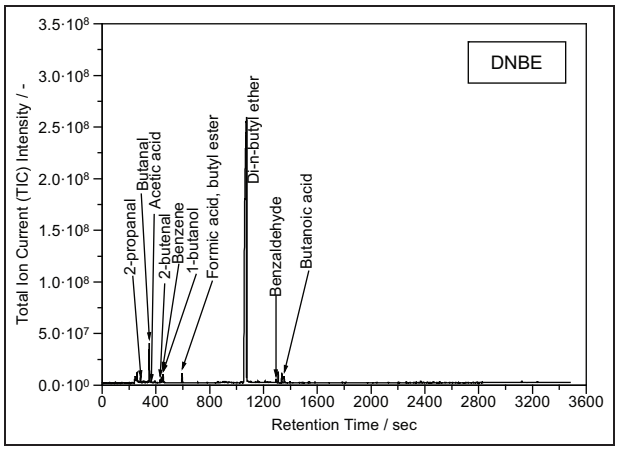

Figure 15. GC-MS HC emission spectra for DNBE at n = 1500 r/min (IMEP = 0.43 MPa) and at EU-6 NO_x level (Tenax).

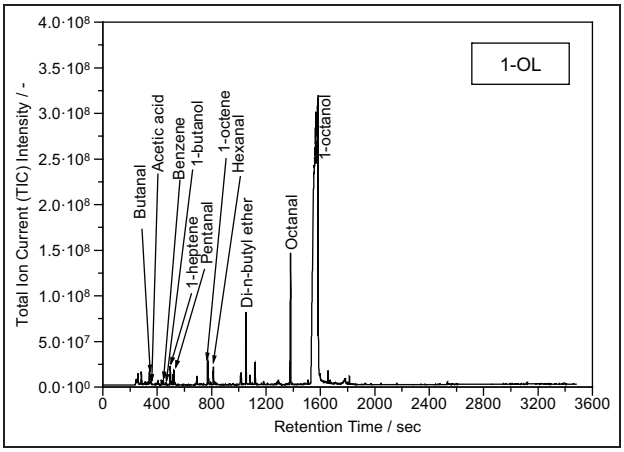

Figure 16. GC-MS HC emission spectra for 1-OL at n = 1500 r/min (IMEP = 0.43 MPa) and at EU-6 NO_x level (Tenax).

unburned fuel. Thus, and contrary to the diesel samples, with both Carbosieve SIII and Tenax tubes, significant peaks in the range of DNBE and 1-OL can be observed. Moreover, in contrast to diesel, in the exhaust gas with TMFBs, slightly more oxygen containing components are detected. Particularly with 1-OL, middle chained alcohols, such as 1-hexanol, are found in the exhaust. Unfortunately, 2-propen-1-ol, which is known to be carcinogenic,[31] can also be traced with DNBE and 1-OL.

In this study, both 1-OL and DNBE showed a purity of $>98\%$. Consequently, the GC-MS analysis with Tenax tube proves that almost no components in the exhaust are found to consist of more than eight carbon atoms. In contrast, diesel is a mixture of a variety of components, including linear alkanes and cyclic structures. In average, diesel fuel has 18 carbon atoms per molecule. For this reason, with diesel fuel, even significant larger molecules, such as n-heptadecane and n-octadecane, are found.

Quantification of toxic hydrocarbon species

By GC-MS analysis, the total quantities of pollutants in the exhaust gas cannot be determined. However, the overall impact of different fuels on specific components in the exhaust gas can be assessed via relative comparison. The adsorbance of the test samples is influenced by the exhaust gas temperature and the water content. Thus, the exhaust gas conditions may vary slightly, even though the engine LP was fixed for all fuels and test samples. The relative adsorbance for each component is expected to be influenced equally. To account for these fluctuations and to allow a relative comparison between the fuels, the area below the graph of the chromatogram is normalized for each species. For the Carbosieve SIII samples, the normalization is carried out by measuring the adsorbance of propene, whereas the adsorbance of the Tenax samples is quantified by measuring benzene. Some of the detected components are known to cause severe damage to the environment and human health. Those are listed in group 1 by the International Agency for Research on Cancer (IARC), thus proven to be carcinogenic to humans.[32] With regard to engine exhaust pollutants, these components are in particular 1,3-butadiene and benzene. However, there are several hydrocarbons found in diesel exhaust gas that are possibly carcinogenic, according to the classification in group 2B. These are in particular acetaldehyde, furan, and ethyl benzene.[32] The quantitative emission analysis with respect to conventional diesel fuel is given in Figure 17 for the LP 1 and in Figure 18 for the LP 2—both at EU-6 NO_x level. The emissions with diesel are set to 100%.

Remarkably, in both LPs, the 1,3-butadiene emissions with DNBE are significantly increased up to 6.5-fold compared to diesel. As shown by Al Rashidi et al.,[33] the scission of the C–O bond at high- and low-temperature combustion is more likely than a scission of a C–C bond. The scission of the C–O bond results in at least one C_4 molecule. Thus, higher emissions of 1,3-butadiene with DNBE are quite reasonable since this

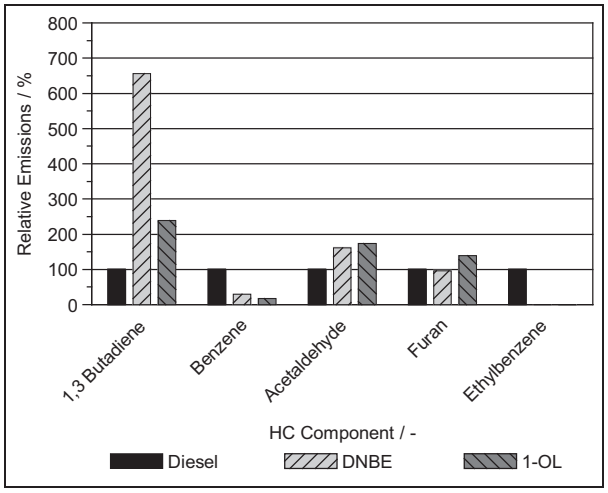

Figure 17. Relative comparison of (probably) carcinogenic emissions at n = 1200 r/min (IMEP = 0.26 MPa) and at EU-6 NO_x level.

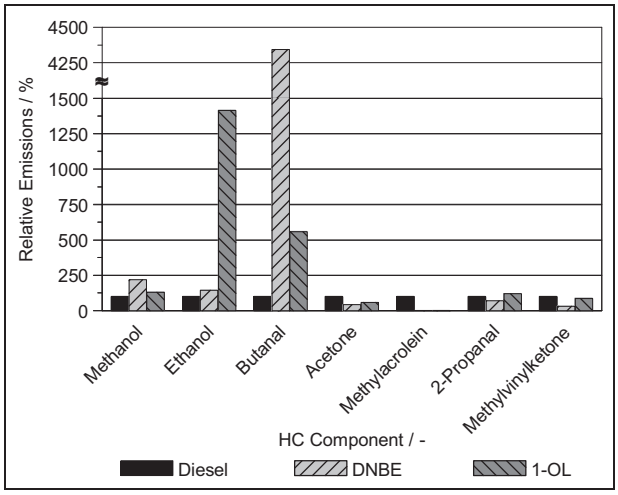

Figure 20. Relative comparison of toxic emissions at n = 1500 r/min (IMEP = 0.43 MPa) and at EU-6 NO_x level.

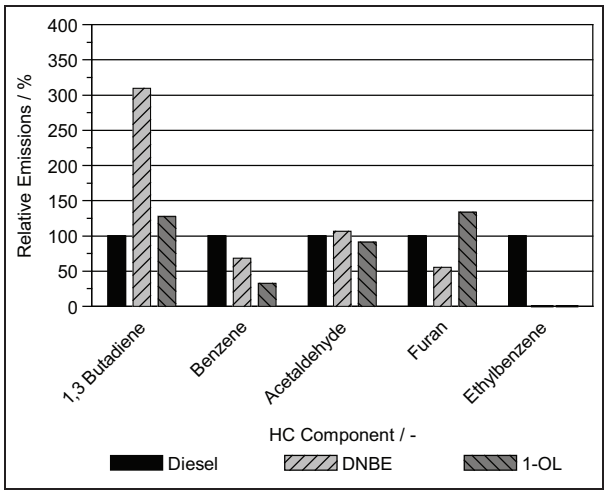

Figure 18. Relative comparison of (probably) carcinogenic emissions at n = 1500 r/min (IMEP = 0.43 MPa) and at EU-6 NO_x level.

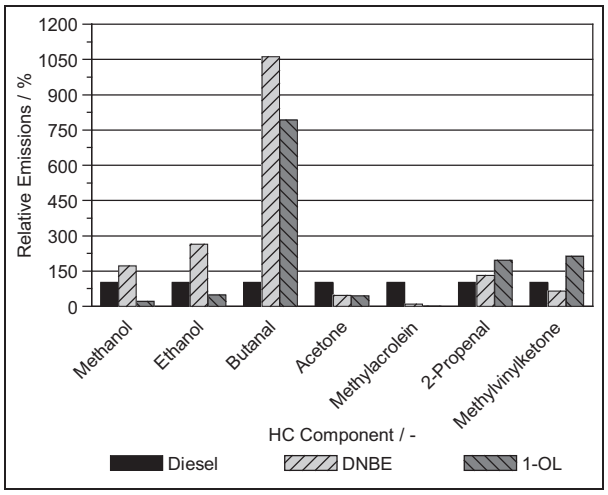

Figure 19. Relative comparison of toxic emissions at n = 1200 r/min (IMEP = 0.26 MPa) and at EU-6 NO_x level.

pollutant is a linear C_4 molecule and, thus, is easily formed during combustion. The emissions of the other carcinogenic hydrocarbons are rather similar to diesel with both the linear C_8 molecules or even below. A major advantage of the utilization of pure, linear molecules is seen in the emission of benzene and ethyl benzene: Since these pollutants are of cyclic structure, the emission of these components is significantly reduced with both the TMFBs. Ethyl benzene is not even traceable in either LPs.

Other components known to be toxic, but not listed by IARC as carcinogenic, are methanol, ethanol, butanal, acetone, methylacrolein, 2-propenal, methylvinylketone, and 2-propen-1-ol. 2-Propen-1-ol was detected with DNBE and 1-OL in low concentrations. However, this component could not be traced on the test samples when diesel was used as fuel. Therefore, a comparative analysis to diesel exhaust is not possible. The emissions of the other listed components are again given on a relative basis to diesel for both oxygenates in LPs 1 (Figure 19) and 2 (Figure 20).

Interestingly, methanol and ethanol emissions with 1-OL are lower than with diesel in the lowest LP, whereas the C_4 molecule butanal exceeds the concentration in 1-OL exhaust by that of diesel exhaust gas. With DNBE, the short-chained alcohol emissions and butanal are found in higher concentrations compared to diesel fuel. The relative emissions of ethanol with 1-OL exceed those with diesel by almost 14-fold, and butanal emissions with DNBE are 43 times higher than with diesel in the LP 2. In both LPs, the emissions of acetone and methylacrolein are reduced substantially with the TMFBs. Methylacrolein is even close to the detection limit with 1-OL in both engine loads tested. For 2-propenal and methylvinylketone, no clear trend can be observed when comparing both LPs and fuels. Nevertheless, the emissions of these species are of the same magnitude for all three tested fuels.

Summary and outlook

In this work, the effect of linear C_8-oxygenates on diesel-type combustion and emissions was studied. Based on SCE experiments with fixed boundary conditions for all three tested fuels, not only the thermodynamic parameters such as heat release rate but also characteristic numbers for assessing the emission reduction potential were determined. The investigations have shown that both oxygenates contribute to a significant reduction in FSN. These results have been validated by EEPS measurements that correlate to the FSN measurements very well and show an overall reduction in total PM up to a factor of 5. Moreover, the particle size shows a substantial shift to lower diameters. Thus, the total PM mass is reduced significantly. Overall, these fuel candidates feature physical and chemical properties that allow an enormous soot reduction without sacrificing, for instance, total CO and HC emissions when compared to diesel. Since the molecular structures are very different to diesel, the composition of the unburned HCs in the exhaust gas was studied in detail by means of Carbosieve SIII and Tenax tubes in combination with GC-MS. These investigations have revealed that the composition is similar for diesel, 1-OL, and DNBE. However, due to 1-OL and DNBE being C_8 molecules, almost no molecules with more than eight carbon atoms were found in the exhaust gas when utilizing these fuels. The major origin of HCs in the exhaust gas at low engine load or cold engine conditions is unburned fuel. For this reason, DNBE and 1-OL were found, which are not existent in diesel exhaust gas. Overall, the quantification, based on a relative comparison, has shown that the emission of carcinogenic compounds is similar for all three types of fuel: On one hand, 1,3-butadiene is found in the exhaust gas of DNBE and 1-OL in higher concentration than that in the case with diesel. On the other hand, ethyl benzene cannot be detected in the exhaust gas with the TMFBs. With regard to toxic, but noncarcinogenic, components, in particular, the emissions of butanal and ethanol were increased compared to diesel. Methylacrolein and acetone were far below the concentrations with diesel fuel. 2-Propenal and methylvinylketone were found to have similar proportions in the exhaust gas as with diesel fuel.

Outlook

With the species in the exhaust gas of the alternative, biomass-based fuels determined, a method will be created to quantify the huge variety of HCs with high accuracy even in transient engine operation by means of FTIR measurement in detail. Moreover, the combustion process will be optimized to reduce the emission of intermediate combustion products with the TMFBs. With the focus on the application of the TMFBs, the impact of high emission of unburned fuel on the aftertreatment system will also be studied.

Declaration of conflicting interests

The authors declare that there is no conflict of interest.

Funding

This work was performed as part of the Cluster of Excellence "Tailor-Made Fuels from Biomass," which is funded by the Excellence Initiative by the German federal and state governments to promote science and research at German universities.

References

1. Dahmen M, Hechinger M, Villeda J and Marquardt W. Towards model-based identification of biofuels for compression ignition engines. *SAE Int J Fuel Lubr* 2012; 5(3): 990–1003.
2. Dahmen M, Villeda J and Marquardt W. Refunctionalization of bio-based platform chemicals into novel biofuels: a computational approach. In: *3rd international conference on sustainable chemical product and process engineering*, Dalian, China, 27–30 May 2013. Dalian, China: Dalian University of Technology.
3. Geilen F, Engendahl B, Harwardt A, Marquardt W, Klankermayer J and Leitner W. Selective and flexible transformation of biomass-derived platform chemicals by a multifunctional catalytic system. *Angew Chem Int Ed* 2010; 49: 5510–5514.
4. Geilen F, vom Stein T, Engendahl B, Winterle S, Liauw M, Klankermayer J and Leitner W. Highly selective decarbonylation of 5-(Hydroxymethyl)furfural in the presence of compressed carbon dioxide. *Angew Chem Int Ed* 2011; 50: 6831–6834.
5. Thewes M. *Potentiale aktueller und zukünftiger Biokraftstoffe für ottomotorische Brennverfahren*. PhD Dissertation, RWTH Aachen University, Aachen, 2014.
6. Heuser B, Kremer F, Pischinger S and Klankermayer J. Optimization of diesel combustion and emissions with tailor-made fuels from biomass. *SAE Int J Fuel Lubr* 2013; 6(3): 922–934.
7. Janssen A, Pischinger S and Muether M. Potential of cellulose-derived biofuels for soot free diesel combustion. *SAE Int J Fuel Lubr* 2010; 3(1): 70–84.
8. Janssen A, Kremer F, Baron J, Muether M, Pischinger S and Klankermayer J. Tailor-made fuels from biomass for homogeneous low-temperature diesel combustion. *Energ Fuel* 2011; 25(10): 4734–4744.
9. Brands T, Huelser T, Hottenbach P, Koss H and Gruenefeld G. Optical investigation of combusting split-injection diesel sprays under quiescent conditions. *SAE Int J Engine* 2013; 6(3): 1626–1641.
10. Kar K, Tharp R, Radovanovic M, Dimou I and Cheng WK. Organic gas emissions from a stoichiometric direct injection spark ignition engine operating on ethanol/gasoline blends. *Int J Engine Res* 2010; 11: 499–513.
11. Ballestoros R, Hernandez J, Loyns L and Tapia A. Speciation of the semivolatile hydrocarbon engine emissions from sunflower biodiesel. *Fuel* 2008; 87: 1835–1843.
12. Montero L, Duane M, Manfredi U, Astorga A, Martini G, Carriero M, et al. Hydrocarbon emission fingerprints from contemporary vehicle/engine technologies with

conventional and new fuels. *Atmos Environ* 2010; 44: 2167–2175.
13. Rounce P, Tsolakis A and York APE. Speciation of particulate matter and hydrocarbon emissions from biodiesel combustion and its reduction by aftertreatment. *Fuel* 2012; 96: 90–99.
14. Bermúdez V, Lujan J, Pla B and Linares W. Comparative study of regulated and unregulated gaseous emissions during NEDC in a light-duty diesel engine fuelled with Fischer Tropsch and biodiesel fuels. *Biomass Bioenerg* 2011; 35: 789–798.
15. Payri F, Bermúdez V, Tormos B and Linares W. Hydrocarbon emissions speciation in diesel and biodiesel exhausts. *Atmos Environ* 2011; 43: 1273–1279.
16. Merritt P, Ulmet V, McCormick R, Mitchell W and Baumgard K. Regulated and unregulated exhaust emissions comparison for three Tier II non-road diesel engines operating on ethanol-diesel blends. SAE paper 2005-01-2193, 2005.
17. Muether M, Lamping M, Kolbeck A, Cracknell R, Rickeard DJ, Ariztegui J and Rose KD. Advanced combustion for low emissions and high efficiency part 1: impact of engine hardware on HCCI combustion. SAE paper 2008-01-2405, 2008.
18. Chang J, Kalghatgi G, Amer A, Adomeit P, Rohs H and Heuser B. Vehicle demonstration of naphtha fuel achieving both high efficiency and drivability with EURO6 engine-out NOx emission. *SAE Int J Engine* 2013; 6(1): 101–119.
19. Thewes M, Mauermann P, Pischinger S, Bluhm K and Hollert H. Hydrocarbon raw emission characterization of a direct-injection spark ignition engine operated with alcohol and furan-based bio-fuels. In: *9th international colloquium fuels conventional and future energy for automobiles*, Technische Akademie Esslingen in Stuttgart, Ostfildern, 15–17 January 2013. Bartz WJ.
20. AVL. *Smoke value measurements with the filter paper method (Application Notes)*. AT1007E, Rev. 02, June 2005, https://www.avl.com/documents/10138//885893//Application+Notes
21. TSIhttp://www.tsi.com/uploadedFiles/_Site_Root/Products/Literature/Spec_Sheets/3090_2980244A.pdf
22. Jakob M, Klein D, Graziano B, Kremer F and Pischinger S. Simultaneous shadowgraphic and chemiluminescent visualization to determine the mixture formation quality and ignition stability of diesel engine related surrogate fuels. In: *14th grazer congress: the working process of the combustion engine*, Graz, Austria, 24–25 September 2013, pp.362–377. Graz, Austria: Graz University of Technology.
23. Internal Test results by ASG analytik-service.
24. Beeckmann J, Aye M, Gehmlich R and Peters N. Experimental investigation of the spray characteristics of di-n-butyl ether (DNBE) as an oxygenated compound in diesel fuel. SAE paper 2010-01-1502, 2010.
25. Heuser B, Laible T, Jakob M, Kremer F and Pischinger S. C8-oxygenates for clean diesel combustion. SAE paper 2014-01-1253, 2014.
26. Song J, Cheenkachorn K, Wand J, Perez J and Boehman AL. Effect of oxygenated fuel on combustion and emissions in a light-duty turbo diesel engine. *Energ Fuel* 2002; 16: 294–301.
27. Vander Wal R and Mueller C. Initial investigation of effects of fuel oxygenation on nanostructure of soot from a direct-injection diesel engine. *Energ Fuel* 2006; 20: 2364–2369.
28. Vander Wal R and Tomasek A. Soot nanostructure: dependence upon synthesis conditions. *Combust Flame* 2004; 136: 129–140.
29. Scott RPW. *Gas chromatography detectors* (Chrom-Ed Book Series), 2003, http://http://faculty.ksu.edu.sa/Dr.almajed/Books/GC.pdf
30. Stuart B. Introduction. In: Stuart B (ed.) *Infrared spectroscopy: fundamentals and applications*. Chichester: John Wiley & Sons, Ltd, 2004, pp.1–13.
31. GESTIS substance databasehttp://gestis-en.itrust.de/nxt/gateway.dll?f = templates$fn = default.htm$vid = gestiseng:sdbeng
32. *Agents classified by the IARC monographs*, vols 1–110 http://monographs.iarc.fr/ENG/Classification/ClassificationsAlphaOrder.pdf
33. Al Rashidi MJ, Davis AC and Mani Sarathy S. Kinetics of the high-temperature combustion reactions of dibutylether using composite computational methods. *P Combust Inst* 2015; 35: 385–392.